ACADÉMIE
DES SCIENCES
INSTITUT DE FRANCE

Comptes Rendus
Chimie

Euphrem Ndayiragije, Prakashanand Caumul, Nausheen Joondan,
Minu Gupta Bhowon and Sabina Jhaumeer Laulloo

L-Tyrosine and L-DOPA: Promising scaffolds for the synthesis of biologically active compounds

Volume 27 (2024), p. 299-317

Online since: 19 November 2024

https://doi.org/10.5802/crchim.342

The Comptes Rendus. Chimie *are a member of the Mersenne Center for open scientific publishing*
www.centre-mersenne.org — e-ISSN : 1878-1543

ACADÉMIE DES SCIENCES
INSTITUT DE FRANCE

Comptes Rendus. Chimie
2024, Vol. 27, p. 299-317
https://doi.org/10.5802/crchim.342

Review article

L-Tyrosine and L-DOPA: Promising scaffolds for the synthesis of biologically active compounds

Euphrem Ndayiragije [a,b], Prakashanand Caumul [a], Nausheen Joondan [a], Minu Gupta Bhowon [*,a] and Sabina Jhaumeer Laulloo [*,a]

[a] Department of Chemistry, Faculty of Science, University of Mauritius, Réduit, Mauritius

[b] Department of Chemistry, Faculty of Science, University of Burundi, Bujumbura, Burundi

E-mails: mbhowon@uom.ac.mu (M. G. Bhowon), sabina@uom.ac.mu (S. Jhaumeer Laulloo)

Abstract. This review reports the synthetic strategies as well as the physicochemical and biological properties of L-tyrosine and 3,4-dihydroxyphenyl-L-alanine (L-DOPA) esters, amides, and imine derivatives including dopamines and tyrosol derivatives from 2010 to 2024. The variations in head group and hydrophilic chain were found to influence the physicochemical properties such as critical micelle concentration (CMC), lipophilicity, and surface tension. The biological properties of the previously reported L-tyrosine and L-DOPA derivatives such as radical scavenging, antibacterial, antiproliferative, and anti-Parkinson activities are also reported.

Keywords. L-Tyrosine, L-DOPA, Physicochemical properties, Biological activities.

Funding. Higher Education Commission (HEC) of Mauritius through Mauritius Africa Scholarship Scheme 2021.

Manuscript received 13 May 2024, revised 5 August 2024 and 12 September 2024, accepted 13 September 2024.

1. Introduction

Aromatic amino acids are an important family of compounds that serve as precursors for the synthesis of many biologically and neurologically active compounds, essential for maintaining normal biological functions. They have been used as building blocks for the synthesis of a number of pharmaceutical compounds. Amino acid based surfactants represent an important class of amphiphilic compounds bearing amino acid residues such as the polar head group coupled to a hydrophobic tail, which have found many applications in pharmaceutical as well as cosmetic and detergent fields [1]. A number of surfactants derived from phenylalanine and tyrosine have been found to possess interesting physicochemical and biological properties, which are influenced by the head group, chain length, as well as the hydrophilicity/lipophilicity balance [2,3]. The tyrosine backbone can be identified in a number of marketed drugs approved by the United States Food and Drug Administration (FDA) [4–6] and has been recognized as a key motif regulating the self-assembly and structural conformation of proteins due to the presence of the phenolic group [7]. A crucial role is played by 3,4-dihydroxyphenyl-L-alanine (L-DOPA) in the therapy of important neurodegenerative disorders such as Parkinson's and Alzheimer's diseases [8,9]. In view of the growing interest in these aromatic amino acids,

*Corresponding authors

the present review reports the synthetic strategies and physicochemical as well as biological properties of L-tyrosine and L-DOPA derivatives.

2. Synthesis of L-tyrosine and L-DOPA derivatives

L-Tyrosine and L-DOPA are aromatic amino acids that consist of a phenolic and a catechol moiety, respectively, and their derivatives belong to a class of bioactive compounds with potential pharmaceutical applications [10]. The presence of carboxylic, amino, and hydroxyl groups allows the possibility of designing multiple structures containing various functional groups such as esters, amides, imines, and functional amines and alcohols (Figure 1).

2.1. *Esters*

L-Tyrosine and L-DOPA ester derivatives are usually synthesized by tethering the α-carboxylic or hydroxyl/phenolic groups. A series of L-DOPA esters **1** have been reported where the α-carboxylic group was esterified by various aliphatic and cyclic alcohols (Figure 2) [11]. The amino group moiety can be further functionalized by protonation or alkylation, yielding cationic ester derivatives. Joondan et al. [2,12] have reported a number of L-tyrosine and L-DOPA alkyl ester hydrochlorides **2** (Figure 2) as well as their quaternary ammonium derivatives **3**. The amino acid esters were synthesized by esterification of L-tyrosine or L-DOPA with fatty alcohols in the presence of *para*-toluene sulfonic acid, followed by reaction with HCl gas to convert the free amine moiety of the esters into hydrochloride salts **2**. However, it was reported that the reaction of the L-tyrosine and L-DOPA esters with bromoethane resulted in ethylation of both the amino and the hydroxyl groups. Cleavage of the *O*-ethyl group with BBr_3 followed by quaternization with methyl iodide gave diethylmethyl ester derivatives **3** (Figure 2) [13]. Aluri and Jayakannan [14] reported the monomeric tyrosine ester–urethane from L-tyrosine for which the amine and carboxylic acid were converted into urethane and carboxylic ester to form the C-methyl ester *N*-methyl carbamate followed by alkylation of the phenolic unit. Polycondensation with polyethylene glycol (PEG) units resulted in tyrosine based poly(ester–urethane)s **4** (Figure 2) [14].

2.2. *Amides*

L-Tyrosine and L-DOPA amide derivatives are generally prepared by functionalizing either the carboxylic or the amino group to give *N*-alkyl amide or *N*-acyl derivatives, respectively (Scheme 1).

2.2.1. *N-Alkyl amide*

The alkylation of the carboxylic moiety of L-tyrosine and L-DOPA usually requires the use of protecting groups. Zhou et al. [15] and Bhunia et al. [16] reported various DOPA alkyl amide derivatives **5** and **6** where the amino and hydroxyl groups were protected by di-*tert*-butyl-dicarbonate (Boc) and benzyl bromide, respectively. Hydrolysis of the *N*- and *O*-protected L-DOPA methyl ester followed by coupling with various amines and then deprotection and acylation gave L-DOPA alkyl amide derivatives **5** and **6** (Scheme 2) [15,16].

The *O*- and *N*-protected Boc-L-DOPA *tert*-butyldimethylsilyl was conjugated with the amino group of lazabemide in the presence of [(1*H*-benzotriazol-1yloxy) tris(dimethylamino) phosphonium hexafluorophosphate] and *N*-methylmorpholine. Cleavage of *O*-Bn and *N*-Boc moieties by using either trifluoroacetic acid or hydrogen chloride gave L-DOPA lazabemide prodrug **7** (Figure 3) [17].

Zhang et al. [18] reported the synthesis of tyrosine based hydroxamic acid **8** via *N*-Boc-protected tyrosine, followed by coupling with phenylamine, and alkylation of the hydroxyl group with methyl bromoacetate. *N*-Deprotection followed successively by acylation of the free amino group with 3-phenylpropionic acid and treatment with NH_2OK in methanol gave tyrosine based hydroxamic acid **8** (Figure 3) [18].

2.2.2. *N-Acyl amide*

N-Acyl L-tyrosine or L-DOPA amide derivatives are obtained by condensation of the amino group with fatty acids through an *N*-acyl linkage and, in most cases, no protecting groups were employed. However, triethylamine (Et_3N) in combination with either other bases or coupling reagents has been used for the *N*-acylation. Triethylamine in the presence of 4-dimethyl-aminopyridine was employed for the condensation of L-tyrosine or L-DOPA ester with fatty acid chlorides with different chain lengths (C10–C18)

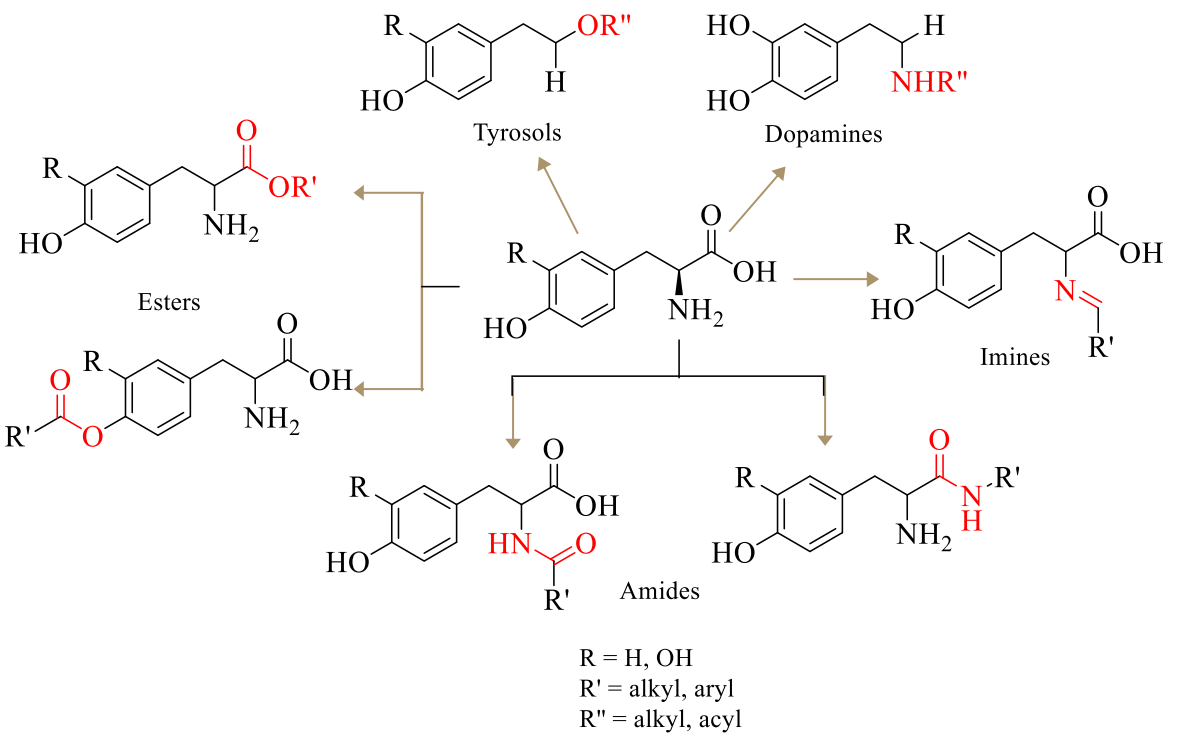

Figure 1. Various types of L-tyrosine and L-DOPA derivatives.

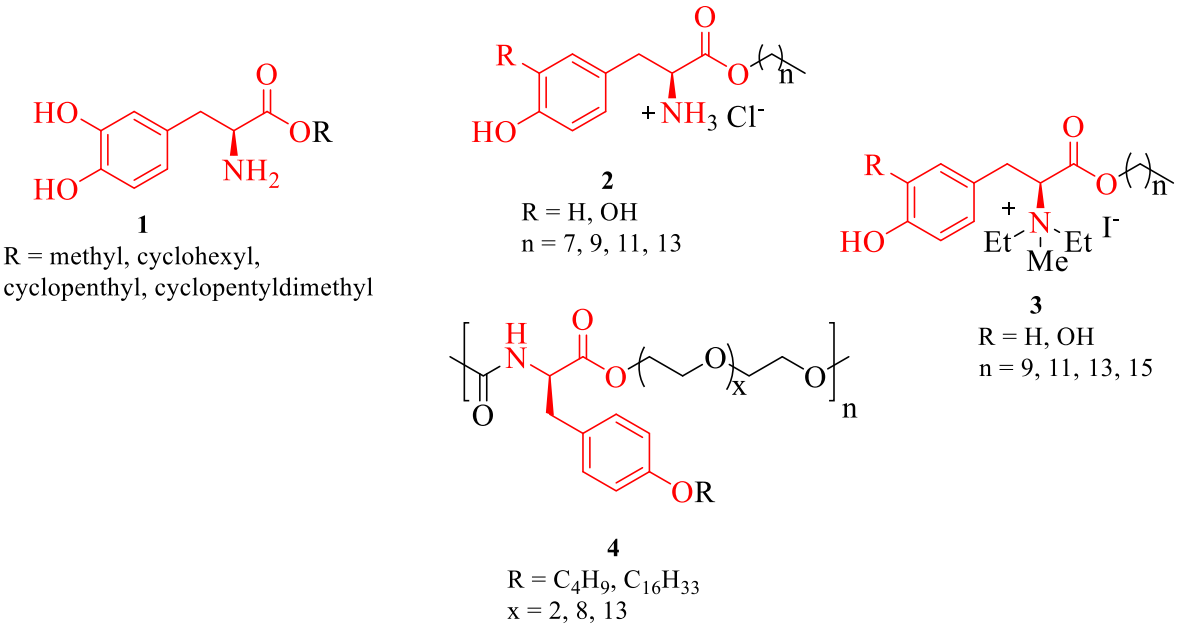

Figure 2. L-Tyrosine and L-DOPA ester derivatives.

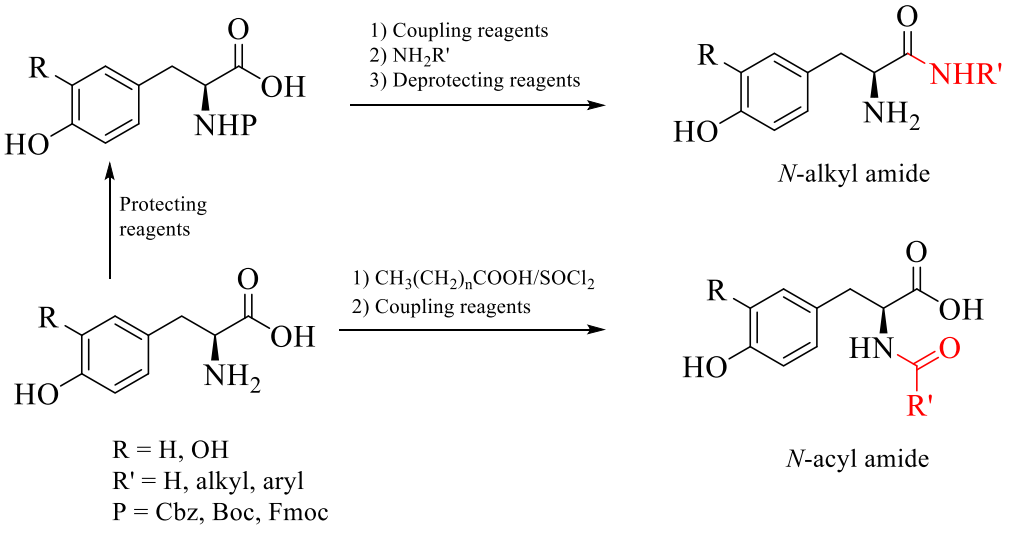

Scheme 1. General synthesis of L-tyrosine/L-DOPA amide derivatives.

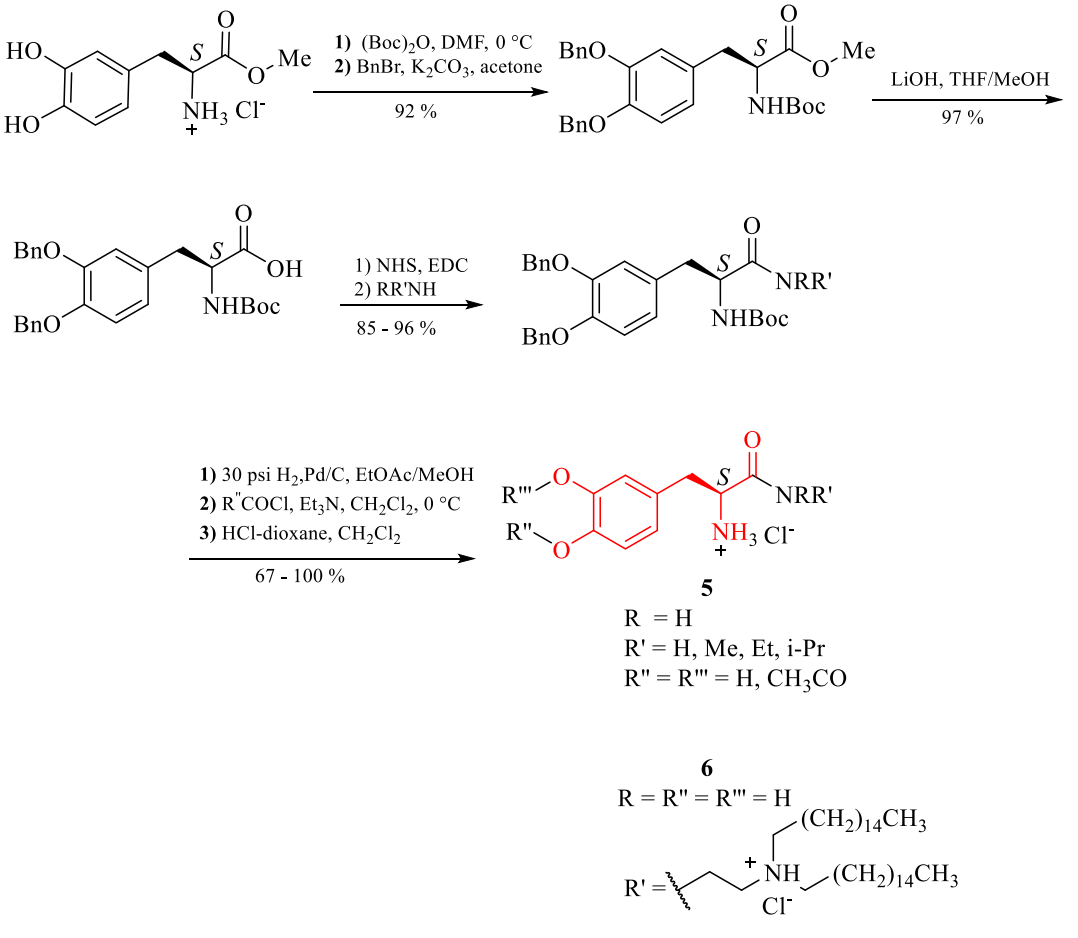

Scheme 2. Synthesis of L-DOPA *N*-alkyl amide derivatives.

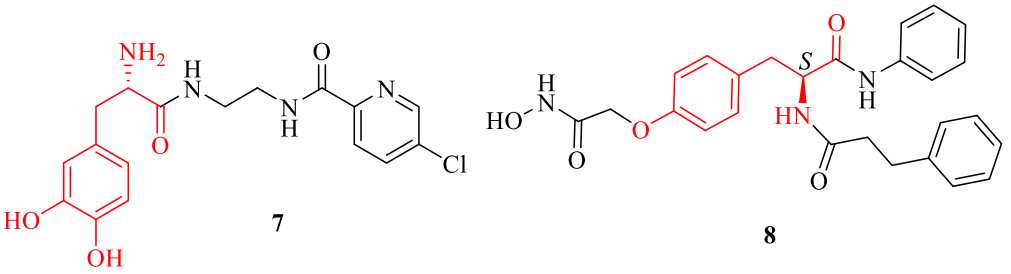

Figure 3. L-Tyrosine and L-DOPA closely related *N*-alkyl/aryl amide derivatives.

to yield the corresponding *N*-acyl monomeric and gemini surfactants **9**–**11** (Figure 4) [19,20].

The coupling of L-DOPA methyl ester with the sulfurated compound [2-methoxy-4-(3-thioxo-3*H*-1,2-dithiol-5-yl)-phenoxy]acetic acid gave L-DOPA amide **12** (Figure 4) [21]. To promote the *N*-acylation in the coupling reaction, Et_3N was used as the catalyst in the presence of coupling reagents, namely *N*,*N*′-dicyclohexyl carbodiimide (DCC) and 1-hydroxybenzotriazole (HOBt). Similar reaction conditions were used for the coupling of diacetyl-L-DOPA-methyl ester hydrochloride with the seleno-L-methionine derivative to give selenyl-L-DOPA derivative **13** (Figure 4) [22]. Dimeric caffeic–L-DOPA **14** (Figure 4) was obtained by the coupling reaction of the trifluoroacetate salt of dibenzyl L-DOPA methyl ester with dimeric acid methyl caffeate, followed by deprotection of the catechol units [23].

Descôteaux et al. [24,25] reported the synthesis of tyrosine–chlorambucil analogues **15a–c**, where chlorambucil is linked to the tyrosine α-amine function by a spacer chain of 5 or 10 carbon atoms (Figure 4). The coupling reaction of L-tyrosine methyl ester hydrochloride or *m*-hydroxyphenyl–tyrosinamide with chlorambucil-6-aminohexanoic or chlorambucil-11-amino-undecanoic acid at the α-amine function gave tyrosine–chlorambucil methyl ester derivatives **15a** and tyrosinamide–chlorambucil derivatives **15c** (Figure 4). Tyrosinol–chlorambucil derivatives **15b** (R = CH_2OH) were obtained from their corresponding tyrosine–chlorambucil methyl esters **15a** (R = CO_2CH_3) by treatment with $LiBH_4$ [24,25].

Tyrosine thiol derivatives **16** were obtained by the reaction of thioester acid derivatives with *O*- and *N*-protected tyrosine whereby the protecting groups di-*tert*-butyl dicarbonate (Boc_2O) and benzyl bromide (BnBr) were used in combination with the coupling reagents hexafluorophosphate benzotriazole tetramethyl uranium (HBTU) and di*iso*propylethylamine (DIPEA). *N*-Boc protection and *O*-benzylation of tyrosine, followed by concomitant methylation and *N*-Boc cleavage, gave benzyl ether tyrosine methyl ester hydrochloride salt. Coupling thioester acid derivatives with benzyl ether tyrosine methyl ester in the presence of HBTU and DIPEA followed by hydrolysis in the presence of a sodium hydroxide solution provided tyrosine based thiol derivatives **16** (Figure 4) [26].

L-DOPA phosphoramidate derivatives **17** (Scheme 3) were obtained by the reaction of benzyl acetyl serinate or threoninate with benzyl-protected L-DOPA in the presence of diphenylphosphite, followed by the cleavage of the benzyl group by catalytic hydrogenolysis [27].

The syntheses of a series of α-methyl-L-DOPA urea derivatives **18** (Scheme 4) were reported by the reaction of α-methyl-L-DOPA with various aryl isocyanates under alkaline conditions [28].

2.2.3. *N-Heterocyclic amide*

N-Heterocyclic moieties are present in various bioactive molecules, and about 60% of small-molecule drugs approved by the FDA in 2020 contain *N*-heterocyclic scaffolds with various ring sizes [29,30].

Giorgioni et al. [31] reported the synthesis of L-DOPA based imidazolinones **19** via peptide formation by the coupling reaction of *O*-dibenzo-, *N*-Boc-protected L-DOPA with glycine methyl ester, followed by *N*-Boc cleavage under acidic conditions. Treatment of L-DOPA-glycyl methyl ester dipeptide with either dimethylketone or diethylketone under alkaline conditions followed by catalytic

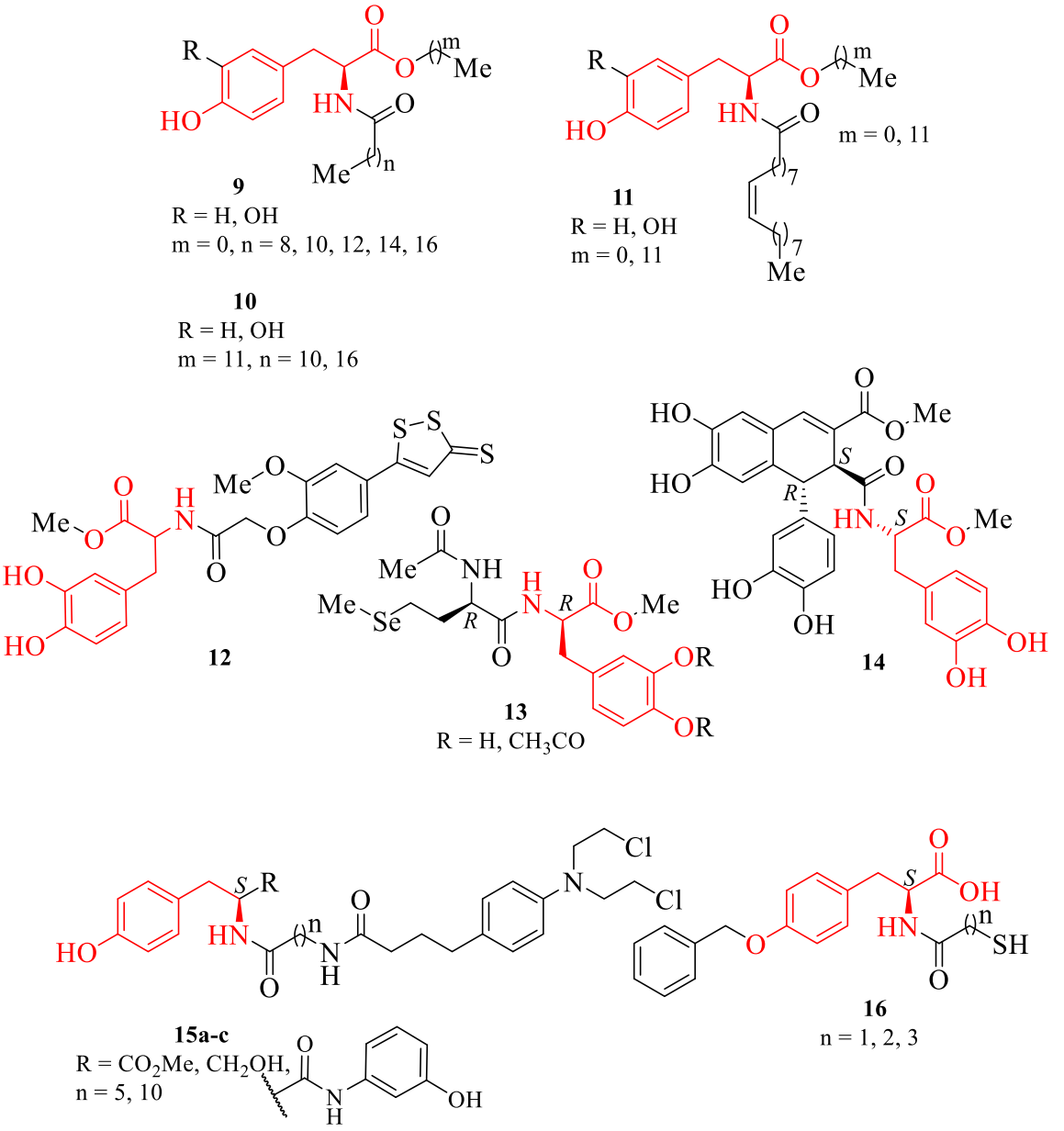

Figure 4. L-Tyrosine and L-DOPA *N*-acyl amide derivatives.

hydrogenation gave L-DOPA imidazolinones **19** (Figure 5) [31].

The reported L-DOPA diketopiperazines **20** (Figure 5) were synthesized by the coupling reaction of *N*-Boc-methionine or *N*-Boc-cysteine derivatives with diaceto-DOPA methyl ester hydrochloride in the presence of triethylamine and *iso*butyl chloroformate (IBCF) followed by deprotection and cyclization [32]. Ravichandran et al. [33] reported the synthesis of L-tyrosine derived hydantoin **21**, which was obtained by the reaction of tyrosine with potassium cyanate in acidic medium.

Treatment of L-tyrosine based hydantoin with methyl methacrylate and 2-hydroxyethyl methacry-

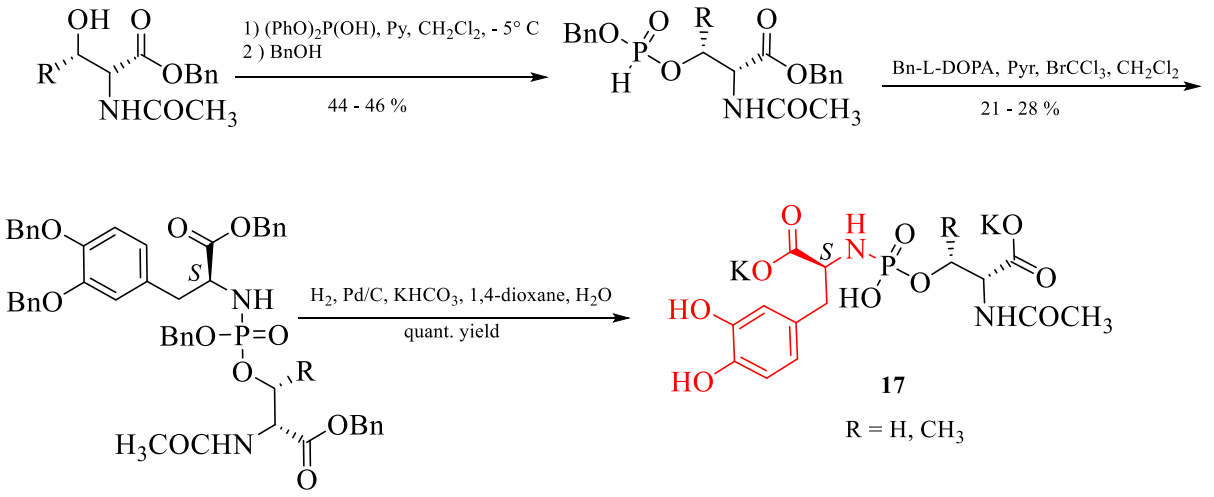

Scheme 3. Synthesis of L-DOPA phosphoramidate with N–P bond.

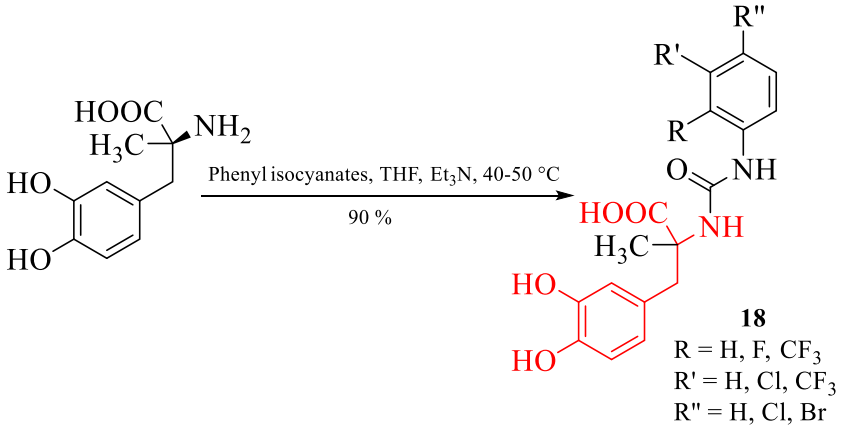

Scheme 4. Synthesis of α-methyl-L-DOPA urea derivatives.

late in the presence of benzoyl peroxide gave vinyl L-tyrosine based hydantoin **21** (Figure 5) [33].

2.2.4. *Peptides*

L-Tyrosine or L-DOPA peptide derivatives consist of compounds containing an L-tyrosine or an L-DOPA moiety linked to another amino acid residue through a peptide bond. Peptides can be synthesized via either a solid or a solution phase, and this strategy proceeds through protection and deprotection of the amino or the carboxylic group. Generally, in peptide synthesis, the use of coupling reagents such as DCC, 1-ethyl-3-(3′-dimethylaminopropyl)carbodiimide (EDC), HOBt, and IBCF is required.

Pinnen et al. [34] reported L-DOPA tetrapeptide derivative **22** (Figure 6) synthesized in solution by an elongation step using fluorenylmethoxycarbonyl (Fmoc) as the protecting group. Deprotection of the *N*-Fmoc-methionylglycyl *tert*-butyl ester using 1,8-diazabicyclo [5.4.0] undec-7-ene and a coupling reaction of the deprotected dipeptide with *N*-acetyl glutamic acid methyl ester in the presence of DCC and HOBt gave the tripeptide *N*-acetyl methyl ester glutamyl-methionylglycyl *tert*-butyl ester. Removal of the *tert*-butyl ester group with trifluoroacetic acid followed by the coupling reaction of the tripeptide with diaceto-DOPA methyl ester hydrochloride in the presence of Et_3N and IBCF gave L-DOPA tetrapeptide derivative **22** [34]. The coupling reac-

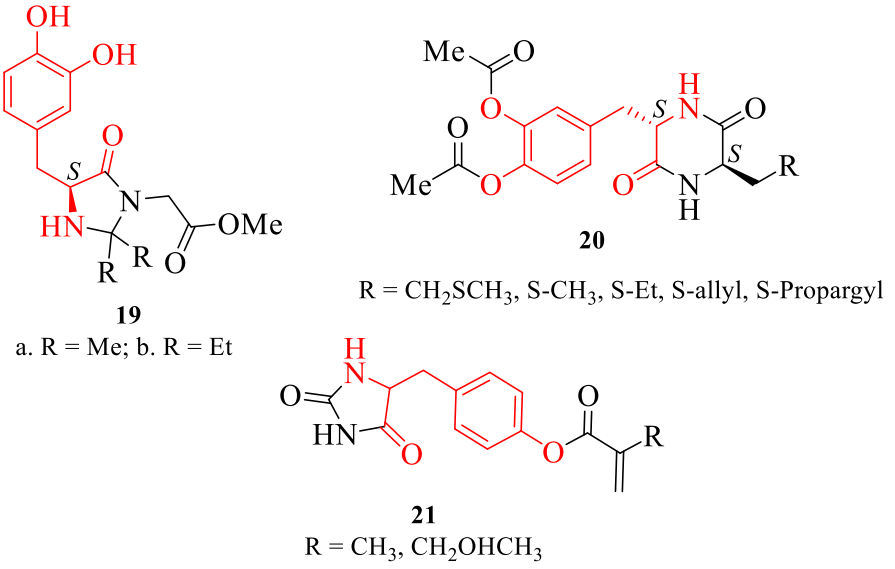

Figure 5. L-Tyrosine and L-DOPA *N*-heterocyclic amide.

tion of L-DOPA esters with *N*-Boc-protected amino acids promoted by EDC and HOBt gave protected dipeptide derivatives, which underwent deprotection by 4 M HCl in dioxane solution to form L-DOPA peptide derivatives **23** (Figure 6) [35]. The natural amide bond formation proceeds usually through protection and deprotection steps, resulting in low yield. An alternative route of the synthesis of peptides with O–C and N–C covalent bonds between amino acid residues, involving Michael-like 1, 4 nucleophilic addition, has been reported by Bizzarri et al. [36]. *Ortho*-hydroxylation of *N*-Boc-Tyr-OMe using 2-iodoxybenzoic acid for oxidative functionalization and reaction with different *N*-Boc-protected amino acids yielded L-DOPA dipeptides **24** and **25** (Figure 6) via the reactive DOPA quinone intermediate [36].

2.3. *Imines*

Schiff bases (CH=N) are found to be versatile pharmacophores for the design and development of various bioactive compounds [37,38]. The synthesis of L-tyrosine and L-DOPA Schiff bases **26** (Figure 7) was carried out by the condensation of *o*-vanillin with L-tyrosine or L-DOPA [39]. Ndayiragije et al. [40] reported the synthesis of L-tyrosine and L-DOPA methyl ester imine derivatives **27** and **28** (Figure 7) by condensation of L-tyrosine and L-DOPA methyl esters with 2-hydroxy-1-naphthaldehyde and 3-*tert*-butyl-2-hydroxybenzaldehyde in the presence of triethylamine [40]. Similarly, the condensation of L-tyrosine with 2-hydroxy-1-naphthaldehyde, methyldopa with 4-dimethylamino-benzaldehyde, and tyrosine with acetylaceto-4-imino-antipyrine in the presence of piperidine yielded imine derivatives **29** [41], **30** [42], and **31** (Figure 7) [43], respectively.

2.4. *Dopamines*

Dopamine is a catecholamine and a neurotransmitter obtained by decarboxylation of L-DOPA [44]. Dopamine plays important roles in the brain and has also been used to prepare numerous drugs [45]. The condensation of 3,4-dimethoxydopamine with cyanuric chloride followed by deprotection of the catechol unit by using BBr_3 gave hexadentate tris(dopamine) **32** (Figure 8) [46]. Condensation of dopamine hydrochloride with 4-hydroxycoumarin or isatin gave dopamine derivatives **33** and **34** [47] while derivative **35** [48] was obtained upon treatment of dopamine hydrochloride with salicylaldehyde (Figure 8).

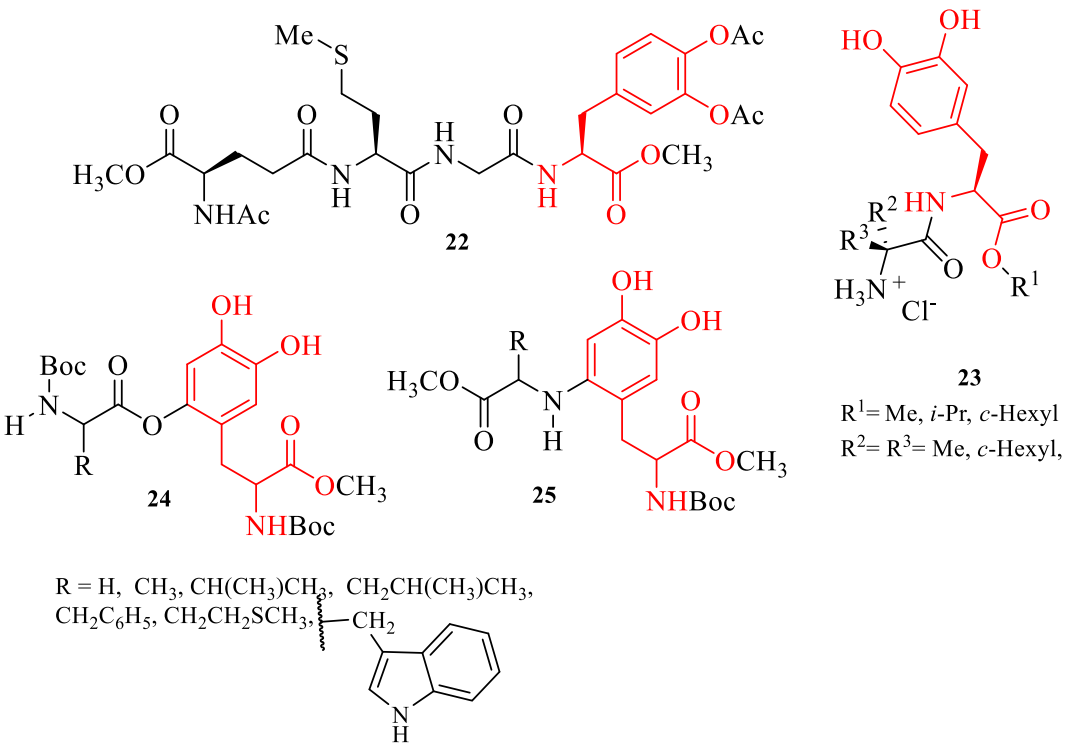

Figure 6. L-DOPA peptide derivatives.

Thakur et al. [45] reported the synthesis of dopamine ester derivative **36** (Figure 8) by the PEGylation process, where the two hydroxyl groups of dopamine were converted to the ester derivative by condensation with ethylene glycol diacid in the presence of H_2SO_4 [45].

2.5. *Tyrosols*

Tyrosols are bioactive compounds and are well known as monophenolic antioxidant compounds. The reduction of tyrosine methyl ester by lithium borohydride ($LiBH_4$) [25] gave tyrosinol, which after deamination formed tyrosol. Acylation at the primary hydroxyl group or regioselective hydroxylation generates tyrosol esters or hydroxytyrosol esters. Tyrosyl/hydroxytyrosol fatty acid esters **37** and **38** were obtained by esterification of tyrosol or hydroxytyrosol with fatty acids in the presence of Novozym 435 biocatalyst (Figure 9) [49–52]. Hydroxytyrosol–lipoic acid ester derivative **39** (Figure 9) was synthesized using an oxidative–reductive process of the esterified tyrosol derivatives using 2-iodoxybenzoic acid followed by in situ reduction with sodium dithionite ($Na_2S_2O_4$) (Figure 9) [53].

3. Biological activities of L-tyrosine and L-DOPA derivatives

L-Tyrosine and L-DOPA derivatives exhibit a wide range of biological activities due to the presence of phenolic and catechol moieties, respectively. The following sections review the biological properties of L-tyrosine and L-DOPA derivatives in terms of radical scavenging, antibacterial, antiproliferative, and bovine serum albumin (BSA) binding activities.

3.1. *Radical scavenging abilities*

Reactive oxygen species (ROS) are produced naturally in the human body during metabolic processes and are required for cellular activities. The generation and inactivation of these ROS are balanced by the natural antioxidants present in the organism [54]. In case of unbalanced biochemical disorders, oxidative stress is activated by the formation of surplus

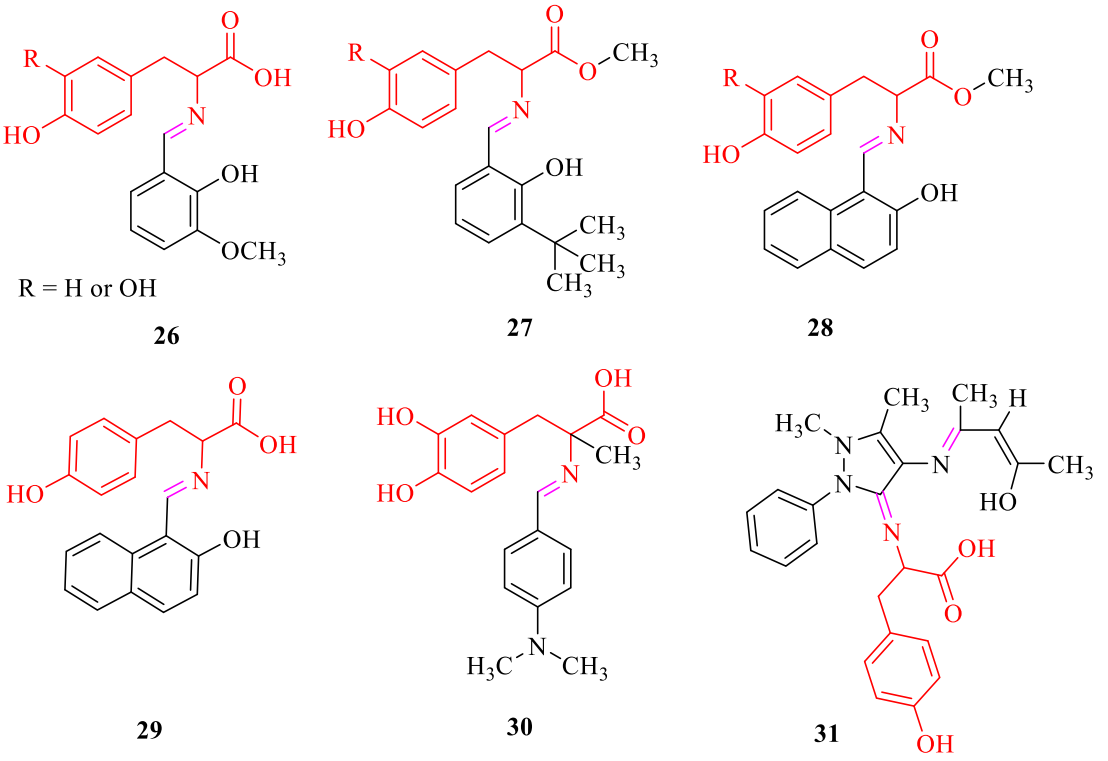

Figure 7. L-Tyrosine and L-DOPA Schiff bases.

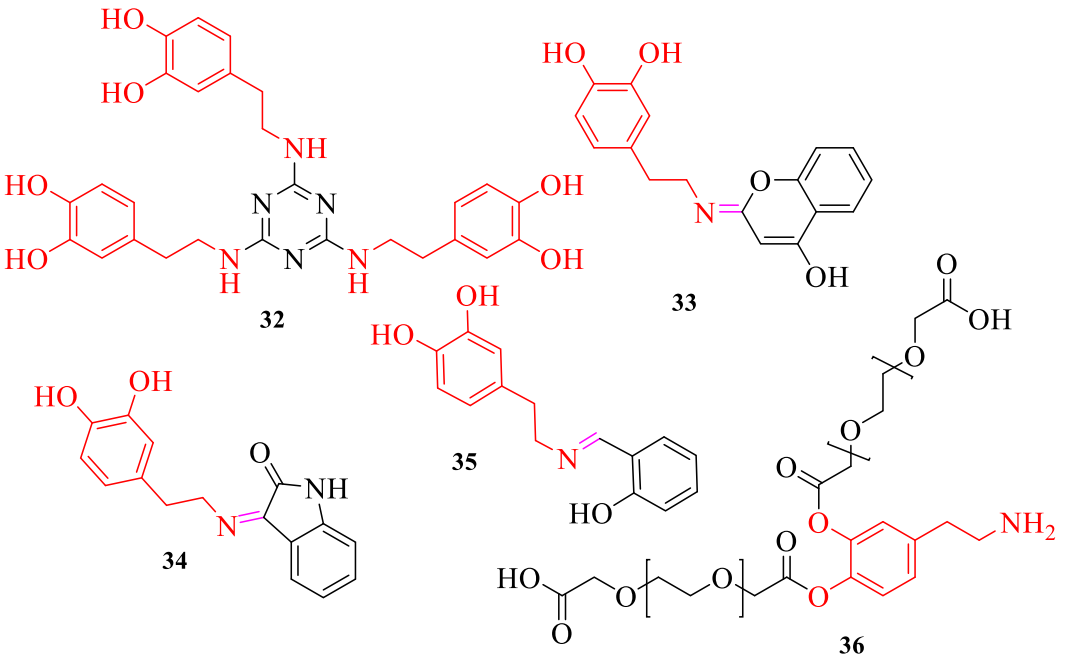

Figure 8. Dopamine derivatives.

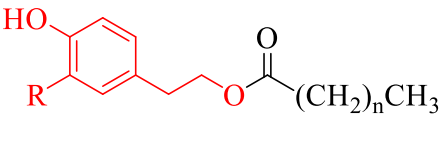

37
R = H, OH
n = 0, 1, 4, 6, 8, 10, 12, 14, 16

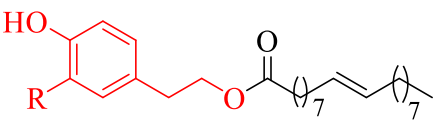

38

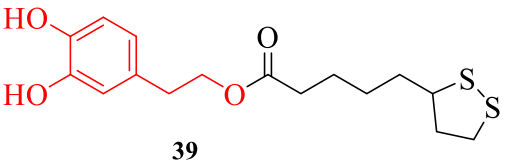

39

Figure 9. Tyrosol derivatives.

amount of ROS produced in vivo, and this leads to neuronal damage and cell death [28]. Antioxidants act as scavengers of the ROS by inhibiting the initiation or propagation of oxidizing chain reactions by donating either hydrogen atoms or electrons to the radicals [55].

In the literature, various methods have been used to evaluate the potential of different antioxidants: 1,1-diphenyl-2-picrylhydrazyl (DPPH) and 2,2′-azino-bis-3ethylbenzo-thiazoline-6-sulfonic acid (ABTS) represent the two most common antioxidants assays used. Reactions with DPPH and ABTS are based on the process of hydrogen atom transfer or electron transfer, where the free radical on the nitrogen atom in $DPPH^{\bullet}$ and the cationic chromophore 2,2-azinobis-(3-ethylbenzothiazoline-6-sulfonate) ($ABTS^{\bullet+}$) are reduced by receiving either a hydrogen atom or an electron from the free radical scavenger [56,57].

Phenolic compounds are known to exhibit strong antioxidant properties in biological systems and protect the human body against neurodegenerative diseases as they donate hydrogen atoms to free radicals. In *ortho*-diphenolic compounds, the intramolecular H-bonding weakens the O–H bond, leading to a lower O–H bond dissociation enthalpy (77.7–80.1 kcal/mol) as compared to phenol (85.1–88.0 kcal/mol), which is responsible for enhancing the radical scavenging abilities [50]. Hence, L-DOPA derivatives containing the catechol moiety exhibit higher activity over their corresponding L-tyrosine derivatives.

The poor lipid solubility of the phenolic compounds limits their use in biological systems. The lipophilicity of these compounds can be improved by introducing alkyl chains through esterification or etherification reactions without changing the reacting site responsible for the antioxidant properties [50]. One study has shown that the antioxidant activity of phenolic compounds can be improved by lengthening the alkyl substituent attached to the phenolic compounds due to the enhanced stabilization of the phenoxy radical resulting from the electron-donating substituent [58]. Giorgioni et al. [31] reported that ethyl DOPA imidazolinone **19b** ($\log P$ = 0.94) exhibited higher radical scavenging abilities over its methyl analogue **19a** ($\log P$ = 0.10). The acylated hydroxytyrosyl ester derivatives were also found to be better radical scavengers than the free hydroxytyrosol [59]. Similar observations were made by Sellami et al. [60], where the acylated dopamine derivatives showed higher ABTS radical scavenging abilities than dopamine [60]. Other researchers revealed a parabolic trend with optimum activity for medium alkyl chain length [12,50,61,62], indicating a cut-off effect normally observed between C8 and C14 alkyl chain lengths. Tofani et al. [62] observed that antioxidant capacity of the alkylated hydroxytyrosol (C6–C10) increases as the alkyl chain increases, with a threshold for the decyl chain, after which further chain extension leads to similar activity, whereas in vivo a drastic decrease in antioxidant capacity was observed. L-DOPA fatty esters **2** were found to follow a similar trend with a cut-off effect for the C12 alkyl chain length, with a DPPH IC_{50} value of 2.08 μg/mL and an ABTS IC_{50} value of 21.19 μg/mL [12].

In other studies, an inverse effect of lipophilicity related to radical scavenging activity was reported [36,63]. L-DOPA dipeptides bearing glycine moiety **24** and **25** demonstrated higher antiradical activity compared to L-DOPA peptide derivatives bearing amino acid residues such as alanine, valine, leucine, phenylalanine, methionine, and tryptophan [36]. The radical scavenging abilities of isoquercitrin esters (C4–C10) decreased with elongation of the acyl chain length in both DPPH and ABTS assays [63].

The presence of unsaturation in the alkyl chain was reported to enhance the radical scavenging activity. Hydroxytyrosyl oleate [59], isoquercitrin oleate [63], dopamine oleate [60], and *N*-acyl-L-DOPA oleyl gemini surfactant [20] were found to exhibit good radical scavenging abilities. This could be attributed to the restriction in conformational freedom resulting from the double-bond rigidity, which disfavors a folded conformation causing a shielding effect of the phenolic moiety [50]. The nature of the substituents attached to the phenolic moiety was also reported to influence the scavenging ability. Compound **18** bearing a trifluoromethyl moiety showed the highest DPPH radical scavenging abilities (IC_{50} = 17.13 μM) and H_2O_2 free radical scavenging activity (IC_{50} = 22.11 μM) in the series of reported L-DOPA urea derivatives [28].

3.2. *Antibacterial activity*

The microbial resistance against antibiotics has encouraged researchers to develop new compounds having enhanced antimicrobial properties against a wide spectrum of pathogenic microbial strains.

L-Tyrosine and L-DOPA derivatives have been found to possess very good antimicrobial effects against a broad range of bacteria due to the presence of the phenolic group [64–66]. The physicochemical properties, structure, and conformation of bioactive compounds have a great influence on their bactericidal activity. Other important factors, such as the hydrophilicity/lipophilicity balance of the biomolecule and the cationic charge density, govern the antibacterial activity of bioactive compounds [67]. Surfactants with different alkyl chains have the ability to solubilize in lipid membranes and are widely used as antibacterial agents due to their interactions with the bacterial cell membrane.

An increase in antibacterial activity depending on the chain length has been reported, where the optimal effectiveness is generally observed at a particular chain length called the cut-off point, usually between 8 and 14 carbons, where the biological activity increases as the alkyl chain increases, however, after reaching a threshold, the biological activity starts to decrease [49,50]. The alkyl tyrosine (C8–C14) and DOPA (C8–C14) ester ammonium hydrochlorides **2** were reported to exhibit antimicrobial activity against a panel of gram positive and gram negative bacteria. The authors reported that compounds were more active against gram positive compared to gram negative strains. The activity was found to increase by increasing the chain length with a cut-off at C12 for gram positive bacteria and C8/C10 for gram negative bacteria. The dodecyl alkyl esters displayed highest antibacterial activity against *S. aureus*, with minimum inhibitory concentration (MIC) value of 2.6 μM for the L-tyrosine and 249 μM for the L-DOPA derivatives [2,12]. The lower antibacterial activity of the DOPA derivatives was attributed to the stability of the intramolecular hydrogen bonding between the two hydroxyl groups, and hence the hydroxyl groups are less labile for further interaction with the bacterial cell membrane.

Cationic surfactants having a positively charged head group are known to interact with the negatively charged bacterial membrane followed by penetration into the nonpolar tail of the lipid bilayer of the membrane causing cell lysis. Quaternary ammonium derivatives **3** of both tyrosine (C10–C16) and DOPA (C10–C16) displayed higher antibacterial activity than their corresponding alkyl ester ammonium hydrochlorides due to the presence of one methyl and two ethyl groups, which increase the hydrophobicity. The tetradecyl alkyl tyrosine showed the highest antibacterial activity against *S. epidermidis* with an MIC value of 1.7 μM while the L-DOPA analogue exhibited an MIC value of 85 μM [13]. The authors also concluded that antibacterial activity was mainly due to their monomers instead of their micelles [2].

Gemini surfactants exhibit higher antibacterial activity than single-chain surfactants depending on various structural features such as the alkyl chain length, spacer chain length, type of amino acid, and the cationic net charge. It was observed that gemini surfactants with a spacer chain of three carbon

atoms and an alkyl chain length of C10–C12 demonstrate optimum antibacterial activity [67]. The *N*-acyl tyrosine gemini surfactant **10** exhibited better antibacterial activity against *B. cereus* compared to its monomeric analogue, with an MIC value of 0.15 mM because of an increase in hydrophobic interaction between the surfactant molecule and the bacterial membrane.

Monomeric surfactant **11** bearing unsaturation in the side alkyl chain showed enhanced antibacterial activities compared to its saturated homologue **9** due to the double-bond rigidity [19]. This was attributed to the right lipophilic/hydrophilic balance and higher solubility.

L-Tyrosine based thiol derivatives **16** exhibited potent metallo-β-lactamase IMP-1 competitive inhibition activity (K_{ic} ranging from 0.086 to 9.39 μM) [26]. PEGylated dopamine ester **36** showed good antibacterial activity against *B. subtilis*, *S. aureus*, *P. aeruginosa*, and *P. vulgaris* with zones of inhibition ranging from 21 to 27 mm, which were comparable to the positive control ampicillin [45]. Lipophilic tyrosyl ester derivatives (C8–C12) **37** exhibited antibacterial activity against *S. aureus*, *S. xylosus*, and *B. cereus* with MIC in the range 3.1–25 μg/mL [49], showing a cutoff effect at C10.

Schiff bases possess good antibacterial properties due to the presence of the azomethine group, which increases hydrogen bonding interactions with the proteins of the bacteria, subsequently inhibiting bacterial growth. Compared to the positive control norfloxacin with MIC = 3.12 μg/mL, the Schiff base based on dopamine and 4-hydroxycoumarin **33** exhibited higher antibacterial activity against *E. coli*, *K. pneumonia*, *B. subtilis*, and *S. aureus*, with MIC values ranging from 3.12 to 12.25 μg/mL, than its homologue **34** bearing isatin moiety, which showed MIC values in the range 6.25–50 μg/mL [47].

3.3. *Antiproliferative activity*

Phenolic compounds possess interesting pharmacological properties, including protective effects against neurodegenerative and cancer diseases. Antiproliferative activity increases with the easy diffusion of biomolecules into cell membranes, which depends on the balance between hydrophobicity and lipophilicity [68–70].

A number of researchers reported potential applications of L-tyrosine and L-DOPA derivatives for the treatment of certain types of cancer. Tyrosine moieties may improve the therapeutic effect of existing anticancer drugs such as chlorambucil. Tyrosine–chlorambucil methyl ester **15a**, tyrosinol–chlorambucil **15b**, and *meta*-hydroxyphenyl–tyrosinamide–chlorambucil derivatives **15c** displayed enhanced cytotoxic effects towards MCF-7 and MDA-MB-231 cancer cell lines compared to chlorambucil. A spacer chain of five carbon atoms between the tyrosine moiety and chlorambucil was found to be beneficial compared to a spacer chain of ten carbon atoms. This effect can be related to the cut-off effect discussed in the previous section, where bioactive molecules demonstrate optimum activity at a particular chain length. Tyrosine–chlorambucil derivatives with a 10-carbon spacer were reported to be inactive against the breast cancer cell lines MDA-MB-231 probably due to the lower solubility arising from the longer alkyl chain. The higher activity and selectivity towards the cancer cell line MCF-7 over the cancer cell line MDA-MB-231 might be attributed to the difference in cell morphologies [25]. The presence of the alcohol functional group improves antiproliferative activity over the ester functional group. Tyrosinol–chlorambucil analogues showed higher activity than tyrosine–chlorambucil methyl ester analogues. This can be attributed to the solubility promoted by the presence of the hydroxymethyl function, which has a great influence on the hydrophilicity/lipophilicity balance [24].

Many studies have shown that acylation and esterification of L-tyrosine and L-DOPA give rise to derivatives with antiproliferative properties especially towards HeLa cells and MCF-7 cells with optimum activity. Tyrosine based poly(ester–urethane) **4** and their nanoparticles were employed as drug delivery (doxorubicin and camptothecin) vehicles in cancer therapy and were found to be more efficient on the cervical cancer cell line (HeLa) compared to free drugs [14]. Tyrosine based hydroxamic acid **8** exhibited greater histone deacetylase (HDAC8) inhibitory activity (IC_{50} = 0.15 μM) compared to the antitumor agent SAHA (IC_{50} = 1.48 μM) and displayed moderate antiproliferative potency towards cancer cell lines such as MDA-MB-231, A549, HCT-116, and HeLa cell nuclear extract [18].

Dimeric caffeic acid–L-DOPA hybrid **13** displayed interesting and equipotent antiproliferative activities (IC_{50} = 1.00 μM) for breast cancer cell lines MDA-MB-231 and MCF-7 [23]. The antiproliferative activity displayed by lipophilic hydroxytyrosol ester **38** against human cervical HeLa cells (IC_{50} = 0.33 mM) was higher compared to the free hydroxytyrosol (IC_{50} = 0.46 mM), which was attributed to the increase in permeability across cell membranes [51]. The antiproliferative activity of hydroxytyrosol can also be enhanced by attaching other bioactive compounds to the primary hydroxyl group through the transesterification reaction. Ester **39** exerted more potent antitumor activity towards the human colorectal adenocarcinoma HT-29 cell line compared to the parent compounds hydroxytyrosol and α-lipoic acid [53].

3.4. *Anti-Parkinson activity*

Parkinson's disease is a progressive neurodegenerative disorder due to the depletion of dopamine levels in the striatum area of the brain. Therefore, the treatment of Parkinson's disease is based on the restoration of dopamine, a neurotransmitter controlling movement in the central nervous system [8].

Since dopamine cannot cross the blood–brain barrier (BBB) and penetrate into the brain due to its large hydrophilicity, peripheral administration of its precursor, L-DOPA, showed beneficial effects in Parkinson's disease therapy [71]. The challenges associated with the prodrug L-DOPA are its short half-life in plasma, poor solubility, and therefore only 1% of the administered L-DOPA can reach the brain [72]. One of the strategies employed to enhance the bioavailability of L-DOPA includes the development of prodrugs by conjugation of L-DOPA with another moiety with the intention of releasing L-DOPA after enzymatic cleavage of the prodrug [9]. Many researchers showed that functionalization of the hydroxyl, carboxylic, and amino groups into L-DOPA ester and amide derivatives improves the pharmacological response of L-DOPA. Diacetylated L-DOPA amide derivatives **5** generated sufficient and more prolonged plasma levels of L-DOPA (C_{max} = 1746 ng/mL; $t_{1/2}$ = 97 min) after its oral administration compared to the prodrug L-DOPA (C_{max} = 4088 ng/mL; $t_{1/2}$ = 75 min) [15].

Lee et al. [21] carried out in vivo studies in the 6-hydroxydopamine rat model, which revealed that L-DOPA derivatives **12** demonstrated therapeutic potential for Parkinson's disease by increasing the level of dopamine in the brain by 2.2-fold [21]. L-DOPA phosphoramidate **17** derived from serinate was found to possess great potential for sustained release of L-DOPA at pH 7.4 with a half-life time of approximately 10 h [27].

In another study, L-DOPA tetrapeptide **22** maintained a higher dopamine level and demonstrated significant bioavailability with a plasma level of 110 μg/mL versus 75 μg/mL shown by L-DOPA for 4 h post administration [34]. L-DOPA dipeptide **23** tested in the 6-hydroxydopamine lesioned rat model, demonstrated higher rotational response than L-DOPA with 149% peak activity of L-DOPA after 10 min of oral administration [35].

Diketopiperazine-containing propargyl moiety **20** displayed enhanced BBB permeability with a permeability coefficient $P_e = 4.87 \times 10^{-6}$ cm/s compared to L-DOPA ($P_e = 0.75 \times 10^{-6}$ cm/s) [32]. These findings demonstrated that the design of an efficient L-DOPA prodrug is a combination of various factors such as lipophilicity enhancement, size and nature of the substituents, type of bond junction, either ester or amide bond, as well as the hydrophilicity/lipophilicity balance.

3.5. *BSA binding abilities*

The potential use of a drug in clinical practice depends on its binding ability to transport proteins. Serum albumins are the major proteins found in the bloodstream (52–62%) [73]. Human serum albumin (HSA) and BSA are largely used in the development of drug delivery systems. Being less expensive and structurally similar to HSA by 76% [74, 75], BSA is considered an appropriate model to study the interaction between bioactive molecules and blood proteins. BSA consists of 583 amino acid residues distributed into three domains (I–III) with a predominantly α-helical content (55–68%). The three domains—domain I with residues (1–195), II (196–383), and III (384–583)—are assembled together by 17 disulfide bridges, forming the pattern of a heart-shaped molecule. Each domain is subdivided into two subdomains, A and B [76–

78]. The binding interaction of BSA with bioactive molecules is generally investigated using various spectroscopic techniques, such as steady-state fluorescence quenching, synchronous fluorescence, UV–visible, FT-IR, and molecular docking studies [79,80]. The main fluorescence emission properties of BSA arise from BSA chromophore residues such as tryptophan (Trp), tyrosine (Tyr), and phenylalanine (Phe) in the ratio Trp (100)/Tyr (9)/Phe (0.5) [79].

As the contribution of phenylalanine is negligible, many researchers prefer to perform fluorescence emission studies by selectively exciting tryptophan residues at 295 nm [81,82] or by exciting both tryptophan and tyrosine residues at 280 nm [79,83, 84]. Some authors reported the contribution of Trp-212 [85–88] whereas others reported Trp-213 [89,90], but both agree on the conclusion that the main binding site of BSA is located in the vicinity of Trp-134 on the surface of subdomain IA and Trp-212 (Trp-213) within the hydrophobic pocket of subdomain IIA. In view of clarifying the major binding sites of biomolecules with BSA, warfarin and ibuprofen have been extensively employed as binding site markers for subdomain IIA (Trp-212/Trp-213) and subdomain IA (Trp-134), respectively [91].

The binding interactions of biomolecules with BSA are indicated by a decrease in intrinsic fluorescence intensity of BSA combined with a red shift [92–94] or a blue shift [83,95] due to changes in the microenvironment of BSA chromophore residues.

The binding affinity of bioactive molecules with serum albumins provides an indication of their distribution through the circulatory system; therefore, bioactive molecules should be able to bind significantly to the serum albumins. However, a stronger binding of a drug molecule with albumin leads to a decrease in the concentration of the drug in plasma, while a weakly bound drug has a shorter lifetime and poor distribution in plasma [96].

Binding constant values in the ranges 10^6–10^8 M^{-1} and 10^3–10^5 M^{-1} witness strong and moderate interactions, respectively, while a binding constant value less than 10^2 M^{-1} gives an indication of a weak BSA binding interaction with biomolecules [82]. In general, a binding constant (K_b) ranging between 10^4 and 10^6 M^{-1} is suitable for drug–carrier complexes within the circulatory system [79,97]. The interaction of L-tyrosine and L-DOPA derivatives with BSA has been reported, where L-tyrosine derivatives interact more efficiently than L-DOPA derivatives.

L-Tyrosine Schiff base **26** showed higher binding affinity ($K_b = 1.11 \times 10^4$ M^{-1}) with BSA compared to L-DOPA Schiff base ($K_b = 0.96 \times 10^4$ M^{-1}) [39]. The trend is in line with the results reported by Ndayiragije et al. [40] for imine derivatives **27** ($K_b = 3.04 \times 10^6$ M^{-1} versus 1.55×10^5 M^{-1}) and **28** ($K_b = 1.77 \times 10^7$ M^{-1} versus 8.41×10^5 M^{-1}) [40]. This can be attributed to the participation of the two hydroxyl groups in intramolecular hydrogen bonding, thereby lowering the availability of the hydroxyl group for further interaction with BSA.

4. Physicochemical properties of L-tyrosine and L-DOPA derivatives

L-DOPA and L-tyrosine derived surfactants are known to exhibit interesting physicochemical properties owing to the presence of the long hydrophobic chain, which is responsible for their applications in the pharmaceutical as well as in the detergency field. In this section, physicochemical properties in terms of critical micelle concentration (CMC), surface tension, and spatial orientation of L-tyrosine and L-DOPA amino acid based surfactants are discussed.

4.1. *Critical micelle concentration*

Amino acid based surfactants have been known for their desirable surface-active properties due to the formation of intra- and intermolecular interactions that contribute to the self-assembly process [98]. Due to their amphiphilic character, surfactants can interact with biological membranes and improve drug permeability [99].

When these amphiphilic compounds are adsorbed at the water interface and reach a certain concentration, where all surfaces are saturated, they self-assemble to form aggregates called micelles [100]. The minimum concentration of the surfactants at which micellar formation starts is called critical micelle concentration. The CMC values can be determined using different techniques such as conductometric method, tensiometry, and fluorescence spectrometry. Ionic surfactants generally possess higher CMC values than nonionic surfactants, but for both types of surfactants, their CMC values mainly depend on various factors such as the length of the

alkyl chain, solvent composition, temperature, and the size of the polar head group. The micellization process of amphiphilic molecules becomes more favorable with elongation of the lipophilic chain or in the presence of a less polar head group, causing a decrease in CMC values. The CMC values of L-tyrosine and L-DOPA based surfactants are reported to decrease when the alkyl chain length increases. L-Tyrosine derivatives **2** show CMC values ranging from 1.940 mM to 0.013 mM (C8–C14) [2] while CMC values of DOPA derivatives **3** range from 1.070 mM to 0.024 mM (C10–C16) [13]. A larger hydrophilic group weakens the interfacial packing. Therefore, micellar formation becomes less spontaneous, leading to higher CMC values [101]. L-DOPA derivatives **3** (C10–C16) exhibit higher CMC values (1.070 mM–0.024 mM) compared to their homologues, L-tyrosine derivatives **3** (C10–C16, 1.038 mM–0.019 mM) [13].

It has been reported in the literature that hydrophobicity constitutes an important factor in causing a decrease in CMC values. Therefore, the hydrophobic part of the molecule can predominate over the polar head group [101,102]. Gemini surfactants, which are dimeric amphiphilic compounds consisting of two hydrophobic and two hydrophilic groups per molecule, micellize much easily compared to single-chain, monomeric surfactants [67]. Gemini tyrosine derivative **10** shows lower CMC values (0.050 mM) compared to monomeric tyrosine derivative **9** (CMC = 0.117 mM) [19].

4.2. *Surface tension*

Surface tension is a physicochemical property of liquids, which is related to the intermolecular forces interacting over a liquid surface area [103]. The surface tension linearly decreases with increase in concentration of surfactants, indicating that surfactants are adsorbed at the air–solution interface. The effectiveness of a surfactant molecule related to the surface tension at the CMC (γ_{cmc}) corresponds to the maximum reduction in interfacial tension.

The presence of an additional hydroxyl group that contributes to an increase in size of the polar head group for L-DOPA derivatives compared to L-tyrosine derivatives increases the effectiveness of hydroxytyrosol decanoate (γ_{cmc} = 28.0 mN/m) compared to tyrosol decanoate (γ_{cmc} = 41.5 mN/m) [52].

The Gibbs surface excess (Γ_{max}) and the minimum area occupied by a surfactant molecule (A_{min}) are two important interfacial parameters determining the adsorption behavior and packing density. The Gibbs surface excess can be calculated from the Gibbs adsorption equation (Equation (1)):

$$\Gamma_{max} = \frac{-1}{2.303 n' RT}\left(\frac{\delta\gamma}{\delta \log C}\right) \quad (1)$$

where R is the gas constant (8.314 J/mol·K), T is the absolute temperature (298 K), C is the surfactant concentration, $\boldsymbol{\gamma}$ is the surface tension, and n denotes the effective number of species in the solution [104,105]. The Gibbs surface excess (Γ_{max}) increases by increasing the surfactant concentration and the alkyl chain length due to stronger hydrophobic/hydrophobic interactions pushing a maximum number of surfactant molecules to the surface [106, 107]. The minimum area occupied by the surfactant molecule (A_{min}) can be calculated from the Gibbs equation (Equation (2)):

$$A_{min} = \frac{10^{18}}{N\Gamma_{max}} \quad (2)$$

where A_{min} is the minimum area per surfactant molecule at the saturated interface and N is the Avogadro number ($N = 6.022 \times 10^{23}$).

Higher values for A_{min} are an indication of poor packing at the interface, and this parameter varies in the opposite manner with Γ_{max}. Hydroxytyrosol octanoate and hydroxytyrosol decanoate showed higher values (C8: A_{min} = 48.4 Å^2, C10: A_{min} = 39.4 Å^2) compared to their corresponding tyrosol derivatives with the same chain length (C8: A_{min} = 35.3 Å^2, C10: A_{min} = 32.0 Å^2). The minimum surface area decreases with elongation of the alkyl chain, resulting in lower values being displayed by L-DOPA/L-tyrosine derivatives with a C10 alkyl chain length (C10: A_{min} = 39.4 Å^2/C10: A_{min} = 32.0 Å^2) compared to L-DOPA/L-tyrosine derivatives with a C8 alkyl chain length (C8: A_{min} = 48.4 Å^2/C8: A_{min} = 35.3 Å^2) [52]. The *N*-dodecanoyl-L-DOPA methyl ester also showed lower values (A_{min} = 6.6 Å^2) compared to the *N*-decanoyl-L-DOPA methyl ester (A_{min} = 6.7 Å^2) [20].

4.3. *Spatial orientation*

The spatial orientation of surfactants in a specific medium may play an integral part in affecting the

biological activity of systems due to the way they penetrate into the cell membrane.

Joondan et al. [13] investigated the change in conformation of a quaternary ammonium derivative of L-tyrosine **3**. Nuclear magnetic resonance (NMR) studies showed a distinct shielding of the protons of both the ethyl and methyl groups attached to the quaternary ammonium moiety due to ring current effect, which suggests the proximity of the aromatic protons with the quaternary ammonium moiety. The authors concluded that the L-tyrosine and L-DOPA quaternary ammoniums adopt a similar conformation in the aqueous layer, whereby the head group includes the quaternary ammonium moiety and the phenolic group. The higher CMC of the L-tyrosine and L-DOPA quaternary ammoniums was attributed to the bulkiness of the head group, which caused less efficient packing of the molecules at the interface [13]. These results were also confirmed by using 2D NMR to determine the spatial orientation of surfactants.

5. Conclusion

The presence of three different functional groups such as carboxylic, amino, and hydroxyl groups on L-tyrosine and L-DOPA backbones offers a possibility of designing and developing multiple structures with potential industrial applications. Physicochemical and biological properties of L-DOPA and L-tyrosine derivatives are affected by the length, the unsaturation of the alkyl chain, and the presence of other functional groups attached to the L-tyrosine or L-DOPA scaffold. The major challenges in the synthesis of L-tyrosine and L-DOPA derivatives lie in the use of various protecting groups as well as low yield of products. Our group is contributing to the synthesis of new L-tyrosine and L-DOPA derivatives with promising physicochemical and biological properties.

Declaration of interests

The authors do not work for, advise, own shares in, or receive funds from any organization that could benefit from this article, and have declared no affiliations other than their research organizations.

Acknowledgments

EN is grateful to the Higher Education Commission (HEC) of Mauritius for the grant of scholarship through Mauritius Africa Scholarship Scheme 2021 and the University of Mauritius for providing research facilities.

References

[1] J. Zhang, Q. Li, S. Wang, G. Zhang, S. He, C. Liu, C. Wang, B. Xu, *Colloids Surf. A: Physicochem. Eng. Asp.*, 2021, **623**, article no. 126743.
[2] N. Joondan, S. Jhaumeer-Laulloo, P. Caumul, *Microbiol. Res.*, 2014, **169**, 675-685.
[3] N. Joondan, S. J. Laulloo, P. Caumul, P. S. Kharkar, *Curr. Bioact. Compd.*, 2020, **15**, 610-622.
[4] D. Al Shaer, O. Al Musaimi, F. Albericio, B. G. De La Torre, *Pharmaceuticals*, 2020, **13**, article no. 40.
[5] J. Han, H. Konno, T. Sato, V. A. Soloshonok, K. Izawa, *Eur. J. Med. Chem.*, 2021, **220**, article no. 113448.
[6] A. Liu, J. Han, A. Nakano, H. Konno, H. Moriwaki, H. Abe, K. Izawa, V. A. Soloshonok, *Chirality*, 2022, **34**, 86-103.
[7] J. Lee, M. Ju, O. H. Cho, Y. Kim, K. T. Nam, *Adv. Sci.*, 2019, **6**, article no. 1801255.
[8] P. Riederer, R. Horowski, *J. Neural Transm.*, 2023, **130**, 1323-1335.
[9] T. Wiesen, D. Atlas, *Cell Death Dis.*, 2022, **13**, article no. 227.
[10] X. Guo, X. Wu, H. Ma, H. Liu, Y. Luo, *Yeast*, 2023, **40**, 214-230.
[11] N. Furukawa, Y. Goshima, T. Miyamae *et al.*, *Jpn. J. Pharmacol.*, 2000, **82**, 40-47.
[12] N. Joondan, S. Jhaumeer-Laulloo, P. Caumul, *J. Surfactants Deterg.*, 2015, **18**, 1095-1104.
[13] N. Joondan, S. Jhaumeer Laulloo, P. Caumul, D. E. P. Marie, P. Roy, E. Hosten, *Colloids Surf. A: Physicochem. Eng. Asp.*, 2016, **511**, 120-134.
[14] R. Aluri, M. Jayakannan, *Biomacromolecules*, 2017, **18**, 189-200.
[15] T. Zhou, R. C. Hider, P. Jenner *et al.*, *Eur. J. Med. Chem.*, 2010, **45**, 4035-4042.
[16] S. Bhunia, V. Vangala, D. Bhattacharya, H. G. Ravuri, M. Kuncha, S. Chakravarty, R. Sistla, A. Chaudhuri, *Mol. Pharm.*, 2017, **14**, 3834-3847.
[17] M. Hoon, J. Petzer, F. Viljoen, A. Petzer, *Molecules*, 2017, **22**, article no. 2076.
[18] Y. Zhang, J. Feng, C. Liu, H. Fang, W. Xu, *Bioorg. Med. Chem.*, 2011, **19**, 4437-4444.
[19] N. Joondan, S. Jhaumeer-Laulloo, P. Caumul, M. Akerman, *J. Phys. Org. Chem.*, 2017, **30**, article no. e3675.
[20] E. Ndayiragije, P. Caumul, N. Joondan, M. G. Bhowon, S. Jhaumeer-Laulloo, *Results Chem.*, 2024, **7**, article no. 101360.
[21] M. Lee, V. Tazzari, D. Giustarini, R. Rossi, A. Sparatore, P. Del Soldato, E. McGeer, P. L. McGeer, *J. Biol. Chem.*, 2010, **285**, 17318-17328.
[22] A. Di Stefano, L. Marinelli, P. Eusepi *et al.*, *Biomolecules*, 2019, **9**, article no. 239.

[23] G. E. Magoulas, A. Rigopoulos, Z. Piperigkou *et al.*, *Bioorg. Chem.*, 2016, **66**, 132-144.
[24] C. Descôteaux, K. Brasseur, V. Leblanc, S. Parent, É. Asselin, G. Bérubé, *Steroids*, 2012, **77**, 403-412.
[25] C. Descôteaux, V. Leblanc, K. Brasseur, A. Gupta, É. Asselin, G. Bérubé, *Bioorg. Med. Chem. Lett.*, 2010, **20**, 7388-7392.
[26] O. K. Arjomandi, W. M. Hussein, P. Vella, Y. Yusof, H. E. Sidjabat, G. Schenk, R. P. McGeary, *Eur. J. Med. Chem.*, 2016, **114**, 318-327.
[27] F. P. Olatunji, B. N. Kesic, C. J. Choy, C. E. Berkman, *Bioorg. Med. Chem. Lett.*, 2019, **29**, 2571-2574.
[28] N. Vadabingi, V. K. R. Avula, G. V. Zyryanov *et al.*, *Bioorg. Chem.*, 2020, **97**, article no. 103708.
[29] R. Banoo, V. K. Nuthakki, B. N. Wadje, A. Sharma, S. B. Bharate, *Eur. J. Med. Chem.*, 2024, **266**, article no. 116131.
[30] N. Long, A. Le Gresley, A. Wozniak, S. Brough, S. P. Wren, *Bioorg. Med. Chem.*, 2024, **98**, article no. 117565.
[31] G. Giorgioni, F. Claudi, S. Ruggieri *et al.*, *Bioorg. Med. Chem.*, 2010, **18**, 1834-1843.
[32] C. Cornacchia, L. Marinelli, A. Di Rienzo *et al.*, *Eur. J. Med. Chem.*, 2022, **243**, article no. 114746.
[33] V. Ravichandran, R. K. Rai, V. Kesavan, A. Jayakrishnan, *J. Biomater. Sci., Polym. Ed.*, 2017, **28**, 2131-2142.
[34] F. Pinnen, I. Cacciatore, C. Cornacchia *et al.*, *Amino Acids*, 2012, **42**, 261-269.
[35] T. Zhou, R. C. Hider, P. Jenner *et al.*, *Bioorg. Med. Chem. Lett.*, 2013, **23**, 5279-5282.
[36] B. M. Bizzarri, C. Pieri, G. Botta, L. Arabuli, P. Mosesso, S. Cinelli, A. Schinoppi, R. Saladino, *RSC Adv.*, 2015, **5**, 60354-60364.
[37] I. Bryndal, M. Stolarczyk, A. Mikołajczyk, M. Krupińska, A. Pyra, M. Mączyński, A. Matera-Witkiewicz, *Int. J. Mol. Sci.*, 2024, **25**, article no. 2076.
[38] M. N. Tahir, M. Ashfaq, K. S. Munawar, A. U. Khan, M. A. Asghar, T. Ahamad, S. C. Ojha, *ACS Omega*, 2024, **9**, 2325-2338.
[39] J. Gao, Y. Guo, J. Wang, Z. Wang, X. Jin, C. Cheng, Y. Li, K. Li, *Spectrochim. Acta - A: Mol. Biomol. Spectrosc.*, 2011, **78**, 1278-1286.
[40] E. Ndayiragije, P. Caumul, N. Joondan, M. P. Akerman, M. G. Bhowon, S. Jhaumeer-Laulloo, *J. Mol. Struct.*, 2023, **1284**, article no. 135352.
[41] İ. Şakıyan, R. Özdemir, H. Öğütcü, *Synth. React. Inorg. Met.-Org. Chem.*, 2014, **44**, 417-423.
[42] L. K. Al-Obidi, T. H. Al-Noor, *J. Pure Appl. Sci.*, 2018, **2017**, 235-247.
[43] V. Soundaranayaki, A. Kulandaisamy, J. Porkodi, *Nucleosides Nucleotides Nucleic Acids*, 2021, **40**, 1050-1074.
[44] P. Andrade-Sampedro, J. M. Matxain, A. Correa, *Adv. Synth. Catal.*, 2022, **364**, 2072-2079.
[45] A. Thakur, S. Ranote, D. Kumar, K. K. Bhardwaj, R. Gupta, G. S. Chauhan, *ACS Omega*, 2018, **3**, 7925-7933.
[46] Q. Zhang, B. Jin, S. Feng, T. Zheng, X. Wang, Z. Guo, R. Peng, *Polyhedron*, 2019, **160**, 261-267.
[47] M.-L. L. Watat, J. S. Chi, C. E. Asanji, E. N. Nfor, *Int. J. Org. Chem.*, 2022, **12**, 40-52.
[48] M. J. Kareem, A. A. S. Al-Hamdani, V. Y. Jirjees, M. E. Khan, A. W. Allaf, W. Al Zoubi, *J. Phys. Org. Chem.*, 2021, **34**, article no. e4156.
[49] I. Aissa, R. M. Sghair, M. Bouaziz, D. Laouini, S. Sayadi, Y. Gargouri, *Lipids Health Dis.*, 2012, **11**, article no. 13.
[50] R. Bernini, F. Crisante, M. Barontini, D. Tofani, V. Balducci, A. Gambacorta, *J. Agric. Food Chem.*, 2012, **60**, 7408-7416.
[51] Z. Bouallagui, M. Bouaziz, S. Lassoued, J. M. Engasser, M. Ghoul, S. Sayadi, *Appl. Biochem. Biotechnol.*, 2011, **163**, 592-599.
[52] R. Lucas, F. Comelles, D. Alcántara, O. S. Maldonado, M. Curcuroze, J. L. Parra, J. C. Morales, *J. Agric. Food Chem.*, 2010, **58**, 8021-8026.
[53] R. Bernini, F. Crisante, N. Merendino, R. Molinari, M. C. Soldatelli, F. Velotti, *Eur. J. Med. Chem.*, 2011, **46**, 439-446.
[54] İ. GülçiN, A. Daştan, *J. Enzyme Inhib. Med. Chem.*, 2007, **22**, 685-695.
[55] I. G. Munteanu, C. Apetrei, *Int. J. Mol. Sci.*, 2021, **22**, article no. 3380.
[56] P. Przybylski, A. Konopko, P. Łętowski, K. Jodko-Piórecka, G. Litwinienko, *RSC Adv.*, 2022, **12**, 8131-8136.
[57] R. Amorati, L. Valgimigli, *Free Radic. Res.*, 2015, **49**, 633-649.
[58] A. Torres De Pinedo, P. Peñalver, J. C. Morales, *Food Chem.*, 2007, **103**, 55-61.
[59] R. Mateos, M. Trujillo, G. Pereira-Caro, A. Madrona, A. Cert, J. L. Espartero, *J. Agric. Food Chem.*, 2008, **56**, 10960-10966.
[60] M. Sellami, A. Châari, I. Aissa, M. Bouaziz, Y. Gargouri, N. Miled, *Process Biochem.*, 2013, **48**, 1481-1487.
[61] M. Laguerre, L. J. López Giraldo, J. Lecomte, M.-C. Figueroa-Espinoza, B. Baréa, J. Weiss, E. A. Decker, P. Villeneuve, *J. Agric. Food Chem.*, 2009, **57**, 11335-11342.
[62] D. Tofani, V. Balducci, T. Gasperi, S. Incerpi, A. Gambacorta, *J. Agric. Food Chem.*, 2010, **58**, 5292-5299.
[63] J. H. Salem, C. Humeau, I. Chevalot, C. Harscoat-Schiavo, R. Vanderesse, F. Blanchard, M. Fick, *Process Biochem.*, 2010, **45**, 382-389.
[64] M. I. El-Gammal, M. I. Abou-Dobara, H. A. H. Ibrahim, S. A. Abdulhafith, M. A. Okbah, *Egypt. J. Aquat. Res.*, 2024, **50**, 71-77.
[65] Z. Li, M. Wu, H. Yan, Z. Meng, B. Gao, Q. Dong, *Foods*, 2024, **13**, article no. 435.
[66] C. E. Maddox, L. M. Laur, L. Tian, *Curr. Microbiol.*, 2010, **60**, 53-58.
[67] A. Pinazo, M. A. Manresa, A. M. Marques, M. Bustelo, M. J. Espuny, L. Pérez, *Adv. Colloid Interface Sci.*, 2016, **228**, 17-39.
[68] L. Dos Santos Oliveira, P. H. De Souza Guarda, L. B. Rosa *et al.*, *Inorg. Chim. Acta*, 2024, **560**, article no. 121806.
[69] M. Feizi-Dehnayebi, E. Dehghanian, H. Mansouri-Torshizi, *J. Iran. Chem. Soc.*, 2022, **19**, 3155-3175.
[70] M. P. Kasalović, S. Jelavca, D. Maksimović-Ivanić *et al.*, *J. Inorg. Biochem.*, 2024, **250**, article no. 112399.
[71] F. Haddad, M. Sawalha, Y. Khawaja, A. Najjar, R. Karaman, *Molecules*, 2017, **23**, article no. 40.
[72] L. B. Vong, Y. Sato, P. Chonpathompikunlert, S. Tanasawet, P. Hutamekalin, Y. Nagasaki, *Acta Biomater.*, 2020, **109**, 220-228.
[73] A. Jahanban-Esfahlan, A. Ostadrahimi, R. Jahanban-Esfahlan, L. Roufegarinejad, M. Tabibiazar, R. Amarowicz, *Int. J. Biol. Macromol.*, 2019, **138**, 602-617.
[74] R. Nabi, S. S. Alvi, M. S. Shah, S. Ahmad, M. Faisal, A. A. Alatar, M. S. Khan, *Arch. Biochem. Biophys.*, 2020, **686**, article no. 108373.

[75] P. Rani, C. S. Kiran, K. R. Priyanka, P. Kumar, S. Kumar, J. Sindhu, *J. Mol. Struct.*, 2022, **1270**, article no. 133939.
[76] A. Banu, R. H. Khan, M. T. A. Qashqoosh, Y. K. Manea, M. Furkan, S. Naqvi, *J. Mol. Struct.*, 2022, **1249**, article no. 131550.
[77] P. Dhara, N. Shah, V. Sundaram, A. Srivastava, A. A. Solovev, Y. Mei, D. A. Gorin, K. K. Dey, *iScience*, 2024, **27**, article no. 109286.
[78] Y. Tanjung, M. Dewi, V. Gatera, M. Barliana, I. M. Joni, A. Chaerunisaa, *Nanotechnol. Sci. Appl.*, 2024, **17**, 21-40.
[79] F. Macii, T. Biver, *J. Inorg. Biochem.*, 2021, **216**, article no. 111305.
[80] B.-L. Wang, D.-Q. Pan, S.-B. Kou, Z.-Y. Lin, J.-H. Shi, *Chem. Phys.*, 2020, **530**, article no. 110641.
[81] A. Aguilera-Garrido, T. Del Castillo-Santaella, Y. Yang *et al.*, *Adv. Colloid Interface Sci.*, 2021, **290**, article no. 102365.
[82] D. Singh, L. Kaur, P. Singh, A. Datta, M. Pathak, A. K. Tiwari, H. Ojha, R. Singhal, *J. Photochem. Photobiol. A: Chem.*, 2023, **437**, article no. 114429.
[83] M. Akram, F. Ansari, I. A. Bhat, K. ud Din, *J. Mol. Liq.*, 2019, **276**, 519-528.
[84] B. Kharpan, A. Shyam, R. Nandi *et al.*, *J. Mol. Struct.*, 2024, **1304**, article no. 137633.
[85] M. F. Ansari, F. Arjmand, *J. Mol. Struct.*, 2024, **1304**, article no. 137692.
[86] M. Fatima, F. Nabi, R. H. Khan, A. Naeem, *Spectrochim. Acta A: Mol. Biomol. Spectrosc.*, 2024, **313**, article no. 124076.
[87] X. Jin, Z. Xu, M. Zhang, W. Jia, D. Xie, *Spectrochim. Acta A: Mol. Biomol. Spectrosc.*, 2024, **308**, article no. 123677.
[88] H. Sheikh-Jalali, F. S. Mohseni-Shahri, F. Moeinpour, *J. Mol. Struct.*, 2022, **1252**, article no. 132222.
[89] I. Bala, K. Singh, R. Kataria, M. Sindhu, *J. Phys. Chem. Solids*, 2023, **175**, article no. 111191.
[90] R. Urvika, I. Sharma, K. A. Kiran, K. Arya, R. Gaba, J. Sindhu, R. Kataria, *Inorg. Chem. Commun.*, 2024, **160**, article no. 111938.
[91] O. A. Chaves, L. S. De Barros, M. C. C. De Oliveira, C. M. R. Sant'Anna, A. B. B. Ferreira, F. A. Da Silva, D. Cesarin-Sobrinho, J. C. Netto-Ferreira, *J. Fluor. Chem.*, 2017, **199**, 30-38.
[92] T. Göktürk, E. Sakallı Çetin, T. Hökelek, H. Pekel, Ö. Şensoy, E. N. Aksu, R. Güp, *ACS Omega*, 2023, **8**, 31839-31856.
[93] V. Manakkadan, J. Haribabu, V. N. V. Palakkeezhillam *et al.*, *J. Mol. Struct.*, 2023, **1285**, article no. 135494.
[94] N. Ngueanngam, B. Jityuti, S. Patnin, P. Boonsri, A. Makarasen, A. Buranaprapuk, *Spectrochim. Acta A: Mol. Biomol. Spectrosc.*, 2024, **310**, article no. 123948.
[95] Q. Zhang, Y. Ni, S. Kokot, *Spectrosc. Lett.*, 2012, **45**, 85-92.
[96] N. Akhtar Virk, A. U. Rehman, A. Shuaib *et al.*, *J. Mol. Struct.*, 2023, **1281**, article no. 135070.
[97] D. Yinhua, M. M. Foroughi, Z. Aramesh-Boroujeni *et al.*, *RSC Adv.*, 2020, **10**, 22891-22908.
[98] R. Bordes, K. Holmberg, *Adv. Colloid Interface Sci.*, 2015, **222**, 79-91.
[99] M. Abdul Rub, D. Kumar, *J. Chem. Eng. Data*, 2020, **65**, 2659-2672.
[100] D. R. Perinelli, M. Cespi, N. Lorusso, G. F. Palmieri, G. Bonacucina, P. Blasi, *Langmuir*, 2020, **36**, 5745-5753.
[101] A. Bagheri, *J. Appl. Chem.*, 2021, **15**, 55-64.
[102] M. G. Gab-Allah, A. H. El-Ged, E. A. Badr, M. A. Bedair, S. A. Soliman, M. F. Bakr, *Egypt. J. Pet.*, 2023, **32**, 27-33.
[103] M. Tariq, M. G. Freire, B. Saramago, J. A. P. Coutinho, J. N. C. Lopes, L. P. N. Rebelo, *Chem. Soc. Rev.*, 2012, **41**, 829-868.
[104] S. Das, B. Naskar, S. Ghosh, *Soft Matt.*, 2014, **10**, article no. 2863.
[105] I. Mukherjee, S. P. Moulik, A. K. Rakshit, *J. Colloid Interface Sci.*, 2013, **394**, 329-336.
[106] C. Das, B. Das, *J. Chem. Eng. Data*, 2009, **54**, 559-565.
[107] K. M. Sachin, S. A. Karpe, M. Singh, A. Bhattarai, *J. Chem.*, 2018, **2018**, 1-17.